UCRL-JC-130302
PREPRINT

Recent Advances in Indirect Drive ICF Target Physics at LLNL

B. A. Hammel
T. P. Bernat
G. W. Collins
S. Haan
O. L. Landen
B. J. MacGowan
L. J. Suter

This paper was prepared for submittal to the
17th International Atomic Energy Agency
Fusion Energy Conference
Yokohama, Japan
October 19-24, 1998

January 13, 1998

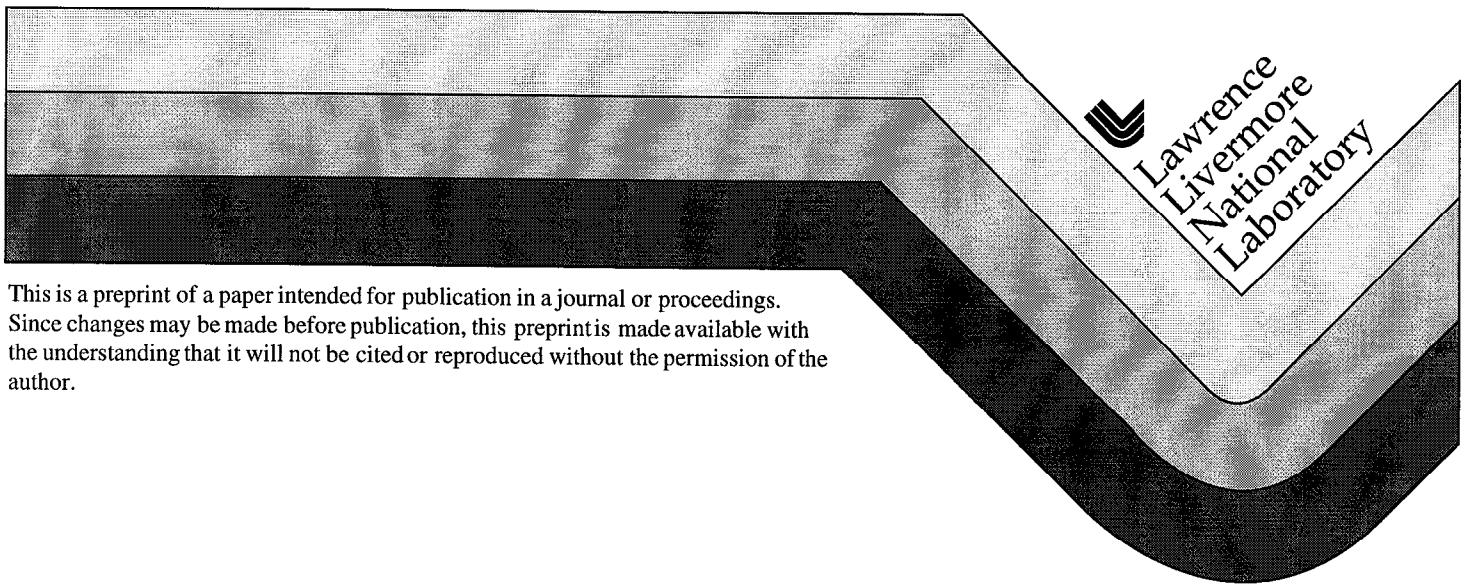

RECENT ADVANCES IN INDIRECT DRIVE ICF TARGET PHYSICS AT LLNL*

B. A. HAMMEL, T.P. BERNAT, G.W. COLLINS, S. HAAN,
O.L. LANDEN, B.J. MACGOWAN, and L.J. SUTER†,
Lawrence Livermore National Laboratory,
Livermore, California 94551
USA

Abstract

In preparation for ignition on the National Ignition Facility, the Lawrence Livermore National Laboratory's Inertial Confinement Fusion Program, working in collaboration with Los Alamos National Laboratory, Commissariat a l'Energie Atomique (CEA), and Laboratory for Laser Energetics at the University of Rochester, has performed a broad range of experiments on the Nova and Omega lasers to test the fundamentals of the NIF target designs. These studies have refined our understanding of the important target physics, and have led to many of the specifications for the NIF laser and the cryogenic ignition targets. Our recent work has been focused in the areas of hohlraum energetics, symmetry, shock physics, and target design optimization & fabrication.

1. INTRODUCTION

In preparation for ignition on the NIF, we are performing a range of experiments on the Nova and Omega lasers to refine our understanding in key areas of target physics. This work is divided into four principal areas; 1) Hohlraum Energetics and the optimization of laser/hohlraum coupling; 2) X-ray drive symmetry and the development of techniques to measure and control it's time dependence; 3) the development of techniques to accurately time the four shock compression of the fuel; and 4) the refinement of ignition capsule designs and the fabrication of cryogenic targets.

2. ENERGETICS

The NIF ignition hohlraum will be heated by 192 laser beams at 0.35 micron wavelength, producing a peak energy of up to 1.8 MJ. We can relate the quantity of x-rays absorbed by a NIF indirect drive ignition capsule, E_{cap}, to the laser energy, E_L, via the expression

$$E_{cap} = \eta_{abs}\eta_{CE}\eta_{HR\text{-}cap} E_L \quad (1)$$

Where η_{abs} is the fraction of incident laser energy absorbed by the hohlraum, η_{CE} is the conversion efficiency of laser light into x-rays and $\eta_{HR\text{-}cap}$ is the fraction of generated x-rays which are actually absorbed by the capsule. η_{abs} is typically assumed to be 1-(fraction of incident light back reflected by stimulated brillioun and raman scattering). Since E_L is nominally 1.8MJ, our standard point design capsules [1] which absorb 150kJ of x-rays require $\eta_{abs}\eta_{CE}\ \eta_{HR\text{-}cap}$=0.083. Additional constraints [2] are that the hohlraum be gas filled; the laser pulse shape be carefully tailored; and the peak radiation temperature (T_r) be 300eV.

* Work performed under the auspices of the U.S. Department of Energy by Lawrence Livermore National Laboratory under contract W-7405-ENG-48.

Numerical simulations of the ignition hohlraum and capsule show a theoretical conversion efficiency, $\eta_{CE,} \sim 0.8$ and a $\eta_{HR\text{-}cap} = 0.14$, producing a theoretical $\eta_{CE}\,\eta_{HR\text{-}cap} = 0.11$. This provides a 25% margin for uncertainties, relative to the required 0.083 coupling efficiency. This uncertainty budget allows us to be off somewhat in our assumptions and still expect to achieve ignition. For example, if $\eta_{abs}=1$ and $\eta_{CE}\,\eta_{HR\text{-}cap} =0.11$ then $E_L=1.35$MJ would successfully drive our ignition design. Or if stimulated backscattering losses proved to be as much as 25% but $\eta_{CE}\,\eta_{HR\text{-}cap} =0.11$, then NIF's expected 1.8MJ will successfully drive the ignition design. Similarly if $\eta_{abs}>0.75$ and $E_L =1.8$MJ, then values of $\eta_{CE}\,\eta_{HR\text{-}cap} <0.11$ would also work.

Given this picture of capsule coupling efficiency, much of our Nova research over the past decade can be broken down into two tasks related to hohlraum energetics: (1) Make η_{abs} as close to 1 as possible in ignition hohlraums; and (2) Test if $\eta_{CE}\,\eta_{HR\text{-}cap}$ is as given by hydro simulations

These Nova experiments and their related analysis indicate that NIF coupling efficiency will meet the requirements for ignition. As we discuss below, ongoing experiments studying stimulated brillouin and raman backscattering (also known as Laser Plasma Interactions or LPI) in NIF "plasma emulators" imply that the total backscattered losses from these two processes should be <10%. Similarly, ongoing experiments examining the radiation environment of Nova hohlraums imply that $\eta_{CE}\,\eta_{HR\text{-}cap}$ will be very close to our expectations from modeling.

2.1. Laser Absorption (η_{abs})

The NIF point design has two cones of beams at angles of ~23 degrees and ~50 degrees entering each laser entrance hole (LEH)[2]. In this design the inner cone at 23 degrees passes through a long path length of HeH_2 gas before striking gold where it converts to x-rays. LPI analysis [3] of ignition hohlraum simulations suggest that the plasma environment important for inner cone backscattering can be approximated on Nova with an ~2.5-3 mm diameter balloon filled with 1 atm of C_3H_8 or C_5H_{12} [4]. Heating such "gas bags" with nine Nova beams produces millimeter scalelengths of plasma of electron density spanning the range of interest for NIF inner beams (0.07-0.1 critical density) at an electron temperature of ~3keV. In these experiments the tenth Nova beam is used as a probe to measure backscattering for the different plasma conditions with a variety of beam conditioning techniques [5] (by beam conditioning we mean modifications to the laser's optical train which "smooth" the intensity distribution at the beam's focal spot).

For NIF's outer cone at 50 degrees, a similar LPI analysis shows that it is most susceptible to backscattering when it interacts with the long scale length gold "shelf" created when gold hohlraum blow-off is tamped by the hohlraum's gas fill. Additional simulations show that this gold shelf can be well emulated on Nova with a standard "scale 1.0" Nova hohlraum (1.6 mm diameter, 2.4 mm long, 1.2 mm diameter LEH's) filled with 1 atm of methane gas and irradiated with a 2.2ns, 3:1 contrast ratio shaped pulse known as ps22. Once again nine Nova beams are used to create the plasma and the tenth is used to explore backscattering with a variety of beam conditioning techniques.

The net result of several years experiments using increasingly refined beam conditioning techniques has been to reduce backscatter losses from our inner and outer cone plasma emulators to levels which we believe are acceptable for NIF. Experiments using our most advanced beam smoothing techniques suggest that the total backscatter losses for the outer cone will be <~5%[5]. Results from Nova gas bag targets, emulating the inner NIF cone, suggest that the total inner beam losses will be <5-10% [5].

On NIF, the outer beams will have ~2/3 of the laser's energy and the inner beams the remaining 1/3. To the degree that the Nova experiments properly emulate the NIF hohlraum plasma and backscattering physics, these LPI experiments suggest that the total losses due to backscattering will be ~(2/3)×5%+(1/3)×(5-10%) for a total of 5-7%. Consequently, we currently estimate that η_{abs}=1-(backscattered fraction) in our NIF point design may well be greater than 90%.

2.2. $\eta_{CE}\,\eta_{HR\text{-}cap}$

We can test our ability to properly predict $\eta_{CE}\,\eta_{HR\text{-}cap}$ by testing our ability to model/predict the relationship between a hohlraum's drive (T_r^4) and the incident laser power, P_L. To see this heuristically, rewrite equation (1) as

$$\eta_{CE}\,\eta_{HR\text{-}cap}\,(\eta_{abs}P_L)=P_{cap}=(1-\alpha_{cap})A_{cap}\sigma\,T_r^4 \qquad (2)$$

Where P_L is the laser power, $P_{cap}=d\,E_{cap}/dt$, A_{cap} is the area of the capsule, α_{cap} is the fraction of incident x-rays re-emitted by the capsule (also known as it's albedo), and σ is the Stephan-Boltzman constant. Thus, for a given capsule of known albedo and area, if we know η_{abs}, then a knowledge of the relationship between laser power, P_L, and T_r^4 gives us knowledge of $\eta_{CE}\,\eta_{HR\text{-}cap}$.

For a number of years experiments have been carried out on Nova [6] and on other facilities to measure, in increasing detail [7], the relationship between P_L and T_r^4. Since 1995 many such experiments have been performed at Nova as part of a collaboration between the US Department of Energy and the French CEA. Under this collaboration we have investigated an extremely wide range of hohlraums and pulse shapes, including gas filled, pulse shaped, ignition-like hohlraums using advanced beam conditioning techniques on all 10 Nova beams [8]. Our most successful technique for measuring hohlraum drive has been to measure the x-ray flux emerging from the laser entrance hole at a modest polar angle (e.g. 22.5 degrees on Nova, 35 degrees on Omega) [9]. For example, Fig. 1 shows a comparison between simulated flux/sr and observed flux/sr exiting the LEH of a methane filled Nova scale 1.0 hohlraum irradiated with a 2.2ns, 5:1 contrast ratio, pulse (ps26). In this case the measured flux was ~10% higher than expected from simulations (in order to simulate this and all other hohlraums in the data base, we reduce the incident laser power by the empirically measured backscatter losses; i.e. η_{abs} is known via measurement). Peak hohlraum drive for this experiment was ~240eV. In all, our time dependent hohlraum drive database includes hohlraums from two facilities (Nova and Omega) which range in temperature from ~110eV to 285eV and have drive pulses between 1 and 6.5ns. Examination of this collection of data leads us to estimate that Lasnex reproduces LEH measurements of time dependent T_r^4 to 4%±7%; i.e., the experimental T_r^4 measurement will be typically contained within a band constructed by taking $1.04\times T_{Lasnex}(t)^4 \pm 7\%$. However, the absolute calibration uncertainty of our principal x-ray flux diagnostic [10] is ±10%. Adding this in quadrature to the ± 7% leads us to conclude that the true T_r^4 will be 1.04±0.12 of Lasnex' T_r^4.

Given this, we conclude that for a given capsule area and albedo, an ignition hohlraum's $\eta_{CE}\,\eta_{HR\text{-}cap}$ will be ~1.04±0.12 of coupling predicted by our simulations. Applying that to the point design gives an estimated coupling of 0.115±0.012.

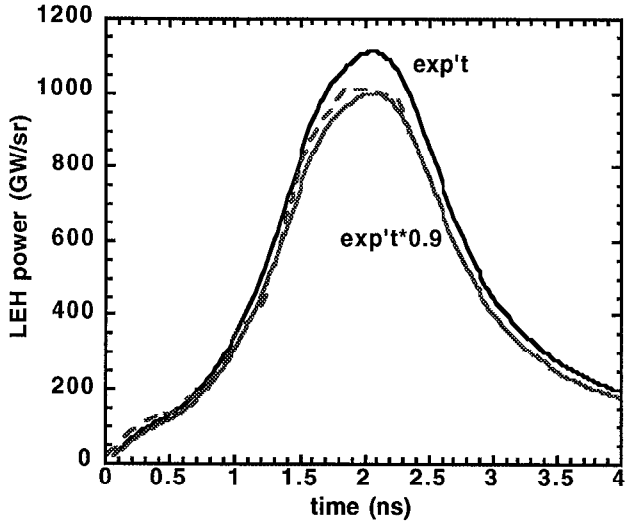

FIG. 1. X-radiation flux/sr from the LEH of a methane filled Nova hohlraum irradiated by "ps26". Solid curves are the measured flux/sr and the measured flux/sr multiplied by 0.9. Dashed curve is the flux/sr from a Lasnex simulation of this experiment.

3. SYMMETRY

In cylindrical hohlraums, flux asymmetries can be decomposed into a Legendre series P_n, with P_2 usually the largest intrinsic asymmetry. The P_2 asymmetry varies in time principally due to motion of the hot laser illuminated rings of plasma as the hohlraum wall blows inward. For x-ray-driven ignition to succeed on the NIF facility, P_2 flux asymmetries imposed on the imploding capsule averaged over any temporal window τ must be maintained below $\approx$ [20/τ (ns)] % [11 12]. The baseline plan for NIF hohlraums is to provide continuous P_2 control (i.e. "beam phasing") by varying the power ratio between at least two sets of beam rings sufficiently separated to cancel the effects of plasma motion. The next order asymmetry, the P_4 moment, must be zeroed out to the <1% level at the capsule by choosing an optimal separation for the beam rings. Higher order asymmetry modes such as P_6 and P_8 are intrinsically smoothed out at the capsule to 1% levels, but the larger hydrodynamic instability growth of perturbations seeded by these shorter wavelength modes limits the tolerable time-integrated P_6 and P_8 to < 0.5%. These conditions place stringent requirements on both measurement accuracy and symmetry control.

Techniques for inferring the flux asymmetries have included recording emission profiles of the hohlraum wall [13], re-emission profiles from high Z spheres [14 ,15] and distortions of surrogate imploding capsules [15] and foam balls [16]. Using these techniques, time-integrated control of P_2 to the 1% level has been demonstrated by appropriate beam pointing in both vacuum [17 ,18] and gas-filled hohlraums [19]. Two recent campaigns conducted at the Omega [20 ,21] and Nova [22] laser facilities have extended the symmetry studies by demonstrating time-dependent control of P_2 and P_4 flux asymmetries. Most recently, a NIF-like multiple ring illumination has been used at Omega to reduce P_2 and P_4 symmetry swings to levels below those required for ignition on NIF. All campaigns [23] used 2-mm scale, 200 eV hohlraums driven by 2.2 ns-long, pulse-shaped 3ω beams with peak powers of 10-20 TW. Time-dependent flux asymmetries were inferred from the shapes of backlit surrogate foam balls. Out-of-round shape deviations at the few micron level are decomposed into Legendre moments which can be differentiated in time to extract flux asymmetry moments.

At Nova, time-dependent symmetry control was achieved by a combination of a) sending different pulses down each half of each beam-line and b) defocusing beams, thus creating two rings of illumination with a time-varying power ratio, but with limited adjustability in ring separation [24].

The measured second order Legendre foam ball distortions are plotted in Fig. 2 for cases with and without different pulse shapes on each half beam. To enhance the effects of the asymmetry swing in the absence of beam phasing, an inner pointing has been deliberately chosen which does not yield a round image at the end of the drive. Fig. 2 clearly shows a greater swing in time in the foam ball distortion in the absence of beam phasing.

For the most recent Omega campaign, a NIF-like multiple ring illumination with adjustable ring separation was exercised. Since the presence of two rings pointed far from the P_2 node position naturally reduces the P_2 symmetry swing, no beam phasing was required. The results from the measured and predicted second and fourth order foam ball distortions are plotted in Fig. 3a and b. Differentiating the data, we infer < 5% P_2 and P_4 asymmetries over any 1 ns interval, below the maximum level tolerable for ignition on NIF. This is to be compared with larger 10% P_2 swings and 4% average P_4 for traditional single pulse, single ring illumination.

As a test of the improved symmetry provided by these multiple cone hohlraums, a series of moderate (10×) and high (20×) convergence implosions were performed. The convergence ratio was varied between 10× and 20× by changing the initial fuel fill pressure from 50 atm to 10 atm D_2. Both low growth factor plain plastic and high growth factor Ge-doped plastic capsule ablators were used. The measured x-ray core image ellipticities were close to round (a/b = 1.1 ± 0.1), in agreement with 2-D simulations. The convergences as measured by a secondary fusion reaction were within 10% of calculated.

The ratio of measured neutron yields to calculated neutron yields from 1D simulations excluding mix and asymmetry effects are plotted in Figure 4 versus measured convergence ratio for these Omega implosions and older Nova implosions with similar pulse-shape and capsule parameters. The recent multiple ring implosion yields from Omega are closer to 1D predictions than the older single ring Nova yields [25 ,26], suggesting better symmetry does improve implosion performance. Moreover, the yield degradation due to the intrinsic even order asymmetries are calculated to be negligible (<5%) for the multiple ring Omega campaigns. The degradation in Omega yields compared to 1D predictions are currently ascribed equally to P_1 asymmetries due to beam-to-beam power imbalances and mix at the pusher-fuel interface. 2-D simulations for these experiments, with mix and asymmetry included, are ongoing.

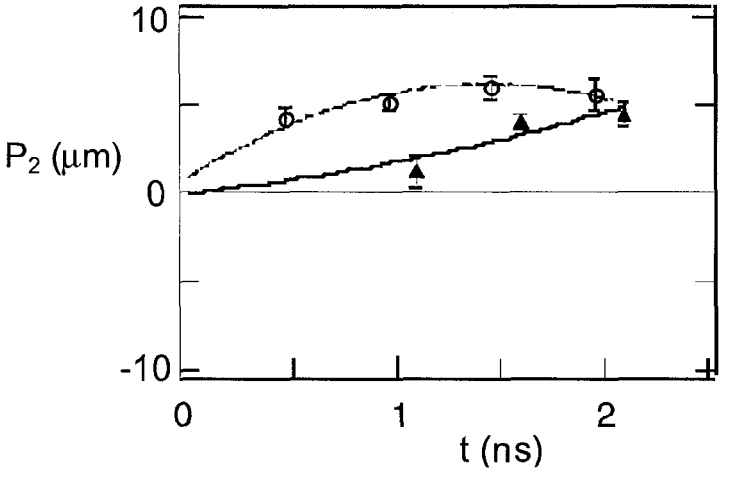

FIG. 2: Results from Nova split beam campaign. Foam ball second order Legendre distortions for phased (triangles) and unphased (open circles) drive. Curves are fits to the data.

Future experiments will better quantify the importance of low order random flux asymmetries on capsule performance. If random asymmetries can be reduced near the level of the intrinsic asymmetries, then we can envisage studying mix effects due to capsule surface roughness in the absence of asymmetry. In addition, we are planning on demonstrating symmetry techniques at the

NIF-scale (6-mm hohlraums). The first 6 to 8 ns of the NIF hohlraum drive can be emulated by Omega and Nova-class lasers. Furthermore, by combining beam staggering with multiple ring illumination, we should be able to minimize P_2 and P_4 asymmetries so that important higher order modes such as P_6 and P_8 can be isolated.

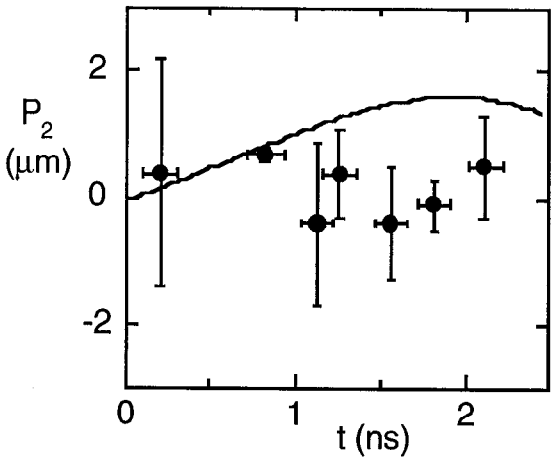

FIGURE 3a

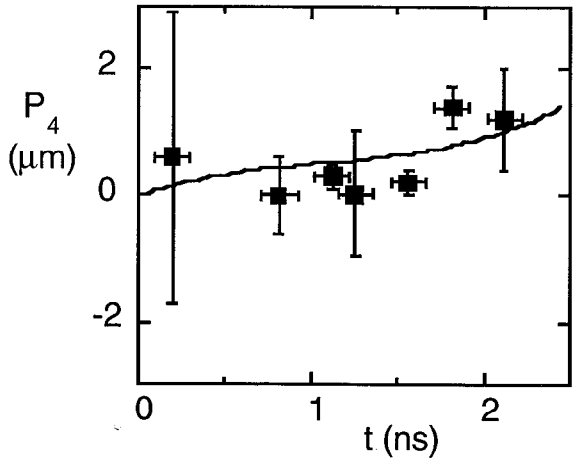

FIGURE 3b

FIG. 3. Results from multiple cone Omega campaign. a) Foam ball second order and b) fourth order Legendre distortions. Curves are calculated distortions.

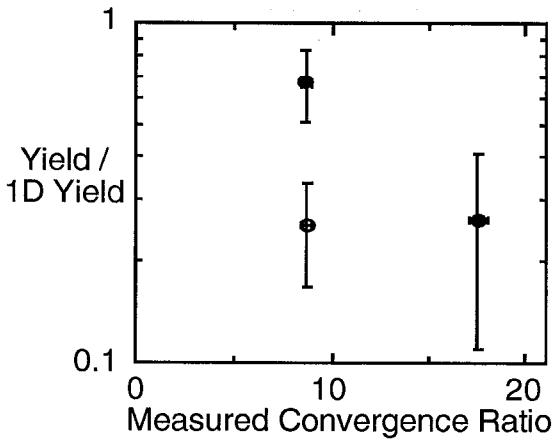

FIG. 4. Ratio of measured to calculated neutron yields vs. measured convergence ratio for multiple ring Omega implosions (closed circles) and Nova implosions (open circles). Both campaigns used 1.2% Ge-doped plastic capsule ablators and a 2.2 ns-long, 6:1 contrast pulse-shaped drive.

4. SHOCK PHYSICS

NIF ignition implosions will require precise laser pulse shaping to achieve the required low isentrope compression of the DT fuel. (FIG. 5).

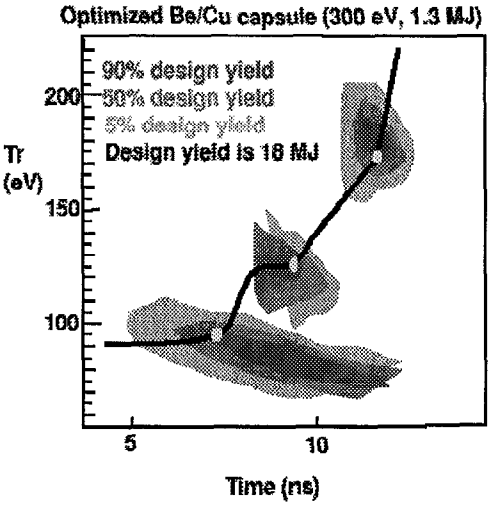

FIG. 5 Sensitivity of shock tuning for an optimized Be/Cu capsule design. Contours show islands of roughly constant yield. Variations in the pulse shape were carried out so as to include only one variation in the optimized shape.

This figure shows the simulated performance for a fully optimized Be/Cu capsule designed for a 300 eV hohlraum drive and 1.3 MJ of laser energy for one specific variation in capsule tuning. Four shocks, each increasing the fuel pressure by ~ 4 and starting with an initial fuel shock pressure of near 0.8 Mbar. Here the change in timing, by say Δt, is performed so as to slide the rest of the pulse shape later in time by Δt. Most of the degradation in capsule performance with miss-timed shocks is due to the increase in fuel entropy. If shocks are timed too close together, shocks converge inside the cold DT fuel and produce a single strong shock. This strong shock heats up the fuel making it difficult to compress. If shocks are timed too far apart, a significant decompression of the fuel occurs after the first shock has passed through the gas solid interface and again the next shock heats up the decompressed fuel through $P\Delta V$ work.

Our approach for timing shocks on NIF is to measure the shock trajectories and to adjust the laser drive for proper shock timing. We will use planar packages on the side of NIF hohlraums to determine the fuel shock trajectory in 1-D and then less sensitive convergent techniques to test the timing of capsules inside the hohlraums. The planar experimental geometry is shown in Fig. 6. As shown we will use both side on radiography and face on velocity interferometry (VISAR) [27] to follow the fuel shock trajectory.

We have tested these techniques in an experiment using a Be pusher directly illuminated with 7.6×10^{13} W/cm^2 at 532 nm. This illumination launches a shock wave in Be which then unloads into deuterium producing a deuterium shock velocity of 33 μm/ns. In the case of radiography, the shock trajectory is measured directly from the streak record. In the case of VISAR, the shock velocity results in a fringe shift, and the shock trajectory is determined by integrating the velocity profile over time. The VISAR data also provides a measure of the shock reflectivity, which is used to understand the transport properties of material at the shock front. The shock velocity from radiography and VISAR are measured to about 2% and <1% accuracy respectively. These techniques, along with less accurate convergent techniques, will provide enough accuracy to properly tune shocks on the NIF.

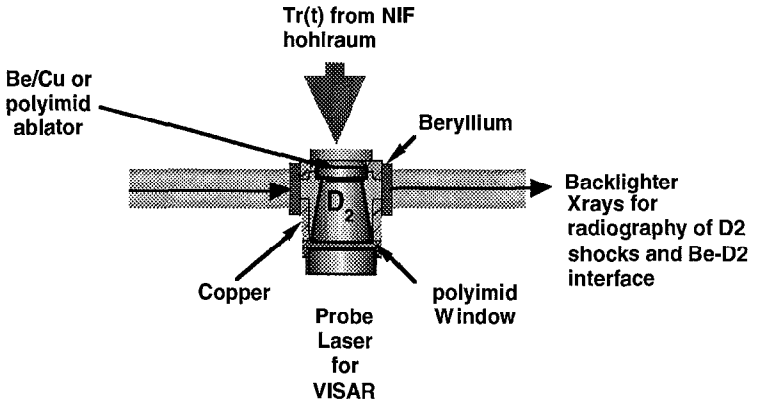

FIG. 6. Schematic diagram of the cryogenic target for radiation driven planer shock timing measurements.

We are also using these experiments to test the equation of state of the fuel and ablator materials required for optimizing ignition capsule designs. In a recent series of experiments we have mapped out the single shock hugoniot for D_2 up to 3 Mbar and tested the single shock hugoniot of CH and Be ablators up to 40 and 15 Mbar respectively.

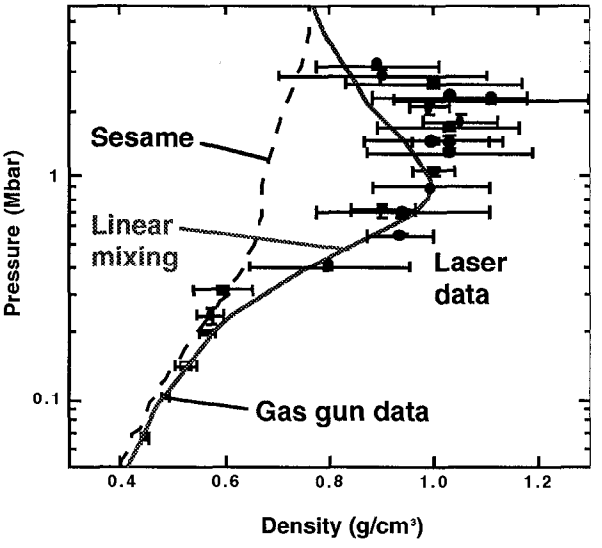

FIG. 7 Deuterium single shock Hugoniot. Dark circles are data taken at the Nova laser facility, open squares are gas gun data, the dashed line is from the Sesame library, and the solid line is a new linear mixing-dissociation equation of state model. The initial density of liquid deuterium is 0.17g/cc at ~ 20 K..

Hugoniot relations do not provide or require temperature which is an important constraint to any equation of state. Temperature determines how much extra work (size of driver) is needed to compress the fuel to the required density. Because of its importance we have also measured the temperature along the single shock Hugoniot and we plot the temperature vs pressure and temperature vs density in Fig. 8 [28]. These data show that the temperature increases very slowly with increasing shock strength up to about 1 eV. This slow increase in temperature with pressure is caused by molecular dissociation and ionization which increase the heat capacity of the fluid, resulting in increased compressibility near 1Mbar and a reduction in the fuel entropy from the first shock in the NIF target design. This "softer" equation of state results in greater margin in ignition designs.

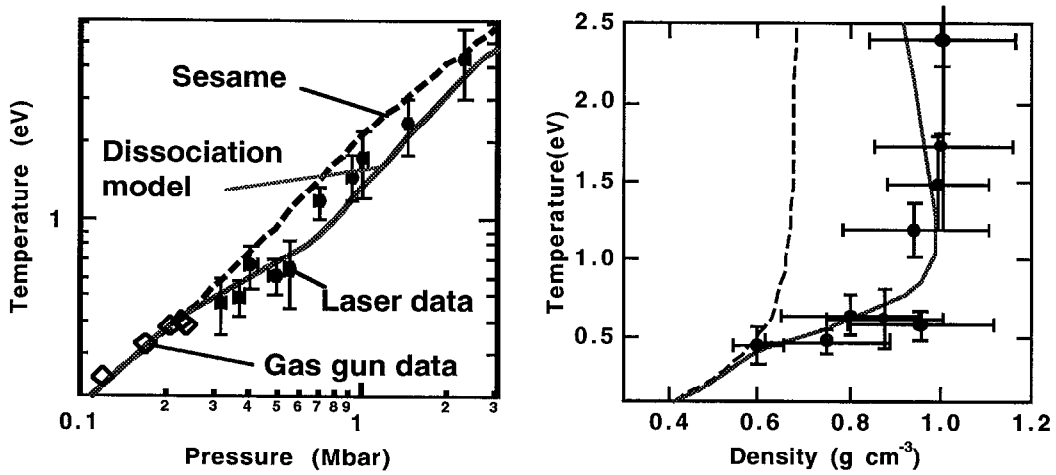

FIG. 8 Deuterium shock temperature along the single shock Hugoniot. Dark circles are data taken at the Nova laser facility, open diamonds are gas gun data, the dashed line is from the Sesame library, and the solid line is a new linear mixing-dissociation equation of state model. The initial density of liquid deuterium is 0.17g/cc at ~ 20 K.

5. IGNITION CAPSULES

Three types of ignition capsules are under development and theoretical investigation: beryllium, polyimide, and CH polymers. A set of 3-dimensional implosion simulations [29] were recently completed for this set of NIF ignition designs. The simulations included imposed capsule and D-T ice surface spectra, based upon measurements of polymer sphere capsules and cryogenic D-T layers observed in cylindrical cells. As seen in Fig. 9, for the same ice roughness and capsule surface roughness, beryllium is superior to polyimide, which is superior to CH. However, while CH capsules have been used over the past decade in both direct and indirect drive experiments, beryllium and polyimide capsule development is not yet complete. We review their status below.

5.1. Beryllium Capsules

There are several reasons for beryllium's superior implosion performance [28] 30]. Beryllium has a lower x-ray albedo and heat capacity than polymers in the temperature range characteristic of NIF hohlraums. This makes Be more efficient and less susceptible to Rayleigh-Taylor instabilities seeded by surface imperfections, as indicated in Fig 9. Its higher density also makes it less susceptible to "feed out" instabilities resulting from roughness perturbations in the frozen DT fuel layer. Its opacity, which is matched to the drive temperature to minimize instability growth and fuel preheat, can be adjusted by adding higher Z dopants. Also, beryllium's strength allows the capsules to hold their fuel charge at room temperature, so cryogenic assembly and handling is not required. Finally beryllium's high thermal conductivity implies that a uniform thickness cryogenic layer may be easier to make (see below). On the debit side, the technique discussed below for enhancing the surface finish of frozen DT layers cannot be applied, and layer characterization is also a much larger problem.

Two methods of fabricating beryllium capsules are being pursued: bonding together micromachined hemishells, at Los Alamos National Laboratory [31], and coating the beryllium onto suitable mandrels by sputter deposition, at Livermore.

In the latter approach, beryllium doped with copper has been sputter deposited onto thin polymer mandrels [32], as shown in Fig 10. Sputtered beryllium is typically columnar in structure, with column widths of a few microns. Such materials typically have less than bulk strength, and the

columnar structure results in high-mode surface roughness. This roughness has been reduced from about 150 nm rms to about 50 nm, measured in a 10 μm surface patch, by substrate biasing of order 120 volts. The bulk columnar structure has been completely eliminated by boron doping at concentrations around 11% [33] as seen in Fig 10. A particular convenience of sputter-deposition is the ease of changing dopant concentrations and types using multiple or specially fabricated sputtering sources, and the ability to produce non-equilibrium material mixtures such as the near-amorphous BeB of Fig 10.

5.2. Polyimide Capsules

The yield sensitivity of polyimide capsules to surface roughness is comparable to beryllium (Fig 9), while its intermediate density (1.4-1.5g/cm^3 compared with about 1 for CH and 1.85 for beryllium) makes it more susceptible to ice roughness than beryllium, but less than for CH. A polyimide capsule potentially has high strength, allowing for room temperature transport with full DT fills [34].

Uniform thickness polyimide ablators are being applied to capsule mandrels by a vapor deposition technique. In this approach the monomer precursors are independently heated under high vacuum to produce monomer vapor fluxes that are directed upon thin-walled capsule mandrels that are being agitated in a pan. The two monomers react on the surface of the mandrels to form a poly (amic acid), which upon further careful heating is converted to polyimide. To obtain high strength coatings it is necessary to carefully balance the vapor fluxes by control of the temperatures of the monomer sources.

To date we have worked with monomers that produce a Kapton-like film [35]. Coating rates are typically 1-2 μm/h. Coatings as thick as 80 μm have been produced, and strengths as high as 100 MPa have been measured. For room temperature transport strengths in excess of 120 MPa are necessary, and we plan to be able to achieve this goal by better control of stoichiometry and coating rate of the monomers, variations in heat treatments, and switching to monomer sources known to produce higher strength polymers. Preliminary investigation of the coating surface finish indicates that reasonably smooth coatings are routinely produced, though localized coating defects sometimes appear that may be related to stoichiometry or deposited debris.

5.3. Cryogenic Fuel Layers

The beta-decay energy deposited in solid D-T drives a phenomenon called "beta layering" in which an irregular formation of solid D-T inside an ICF capsule evolves into a spherically symmetric layer. For "clean" (no ^{3}He present) D-T at the triple point (19.8 K), there is an exponential approach to perfect symmetry with a time constant ≈ 25 minutes.

As discussed for Fig. 9, the performance of an ignition target depends upon the modal spectrum of the inner D-T ice surface, although less sensitively than the capsule outer surfaces. This spectrum, and methods to control it, are currently being investigated. Beta-layered surfaces have been examined in spherical polymer capsules with a very small fill tube for introducing the D-T [36]. We have found that layers with surfaces smooth enough to ignite in 2 and 3 dimensional simulations in any of the capsule materials can be formed, as seen in Fig 11(a). In Fig 11(b), the surface spectrum taken from shadowgraphs is compared with the spectrum used in the simulations of Fig 9. Those simulations used only the portion of the spectrum above mode 15. To obtain this layer quality in spheres, the initial layer must be developed from a single nucleation point, which requires avoiding severe supercooling. Similar surface spectra have been obtained in cylindrical experiments [37].

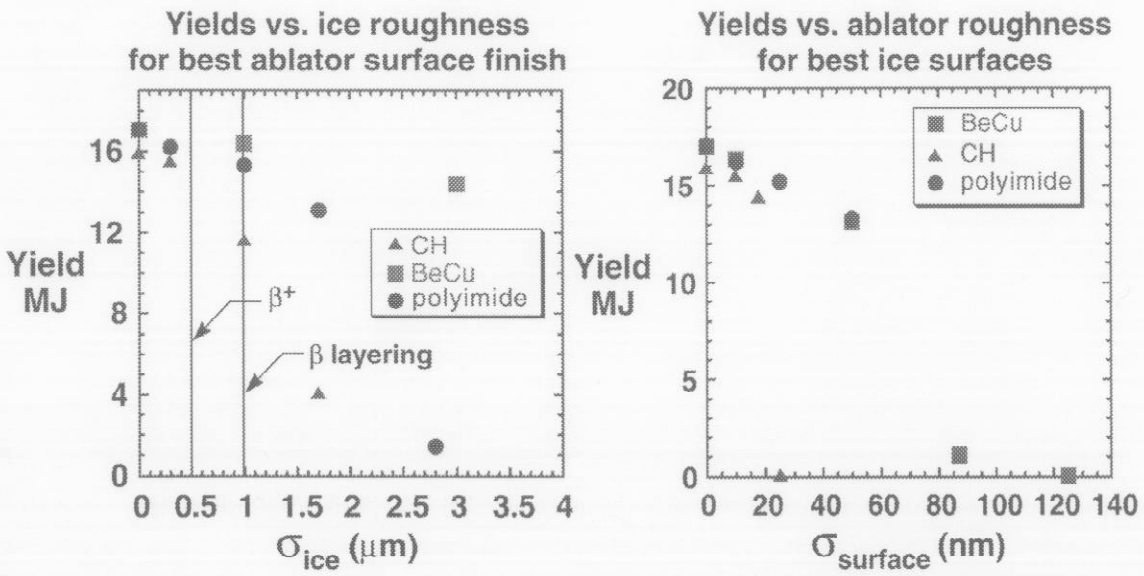

(a) *(b)*

FIG. 9 (a) Yield vs. ablator rms surface roughness for the best ice surfaces obtainable (1 μm for beryllium, 0.5 μm for polymers using auxiliary smoothing techniques). The rms is derived from the model spectrum of fig. 11(b), using model 1 to 120. Ice roughness from natural β layering is approximately 1μm, and enhanced smoothing by infrared absorption (β+) may give 5μ m rms. (b) Yield vs. ice roughness for the best rms outer surface roughness (10 nm).

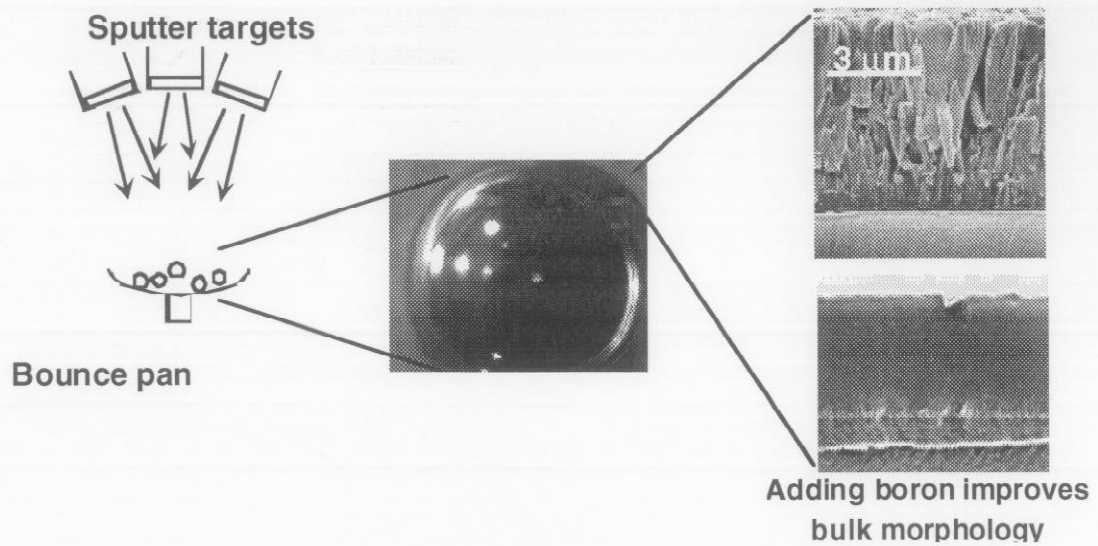

FIG. 10 Sputter deposition approach for fabricating beryllium ignition capsules.

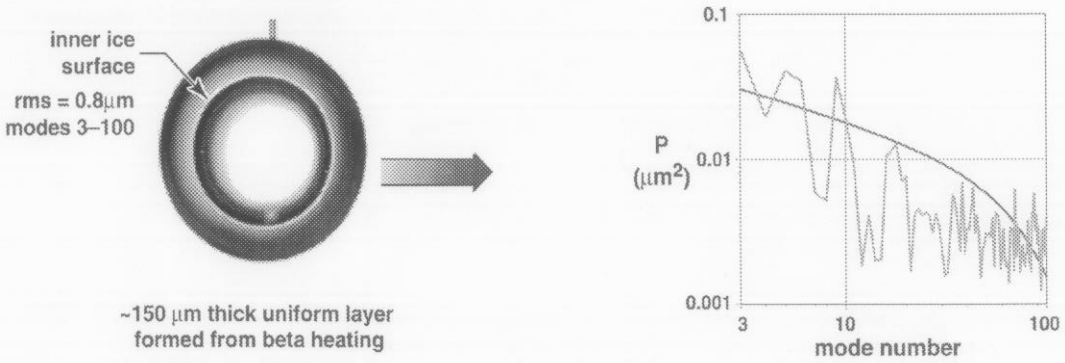

FIG. 11 (a) A shadowgram of a very smooth D-T layer formed by beta-layering in a very thin (approximately 10 μm) polymer shell; (b) the surface spectrum from (a) compared to that used in the simulations of Fig 9.

The fuel layer smoothening by beta heating is halted by the surface energies of the multicrystalline surfaces. However, smoother surfaces would increase confidence in ignition on the NIF by allowing for uncertainties in the simulations and variations in the surface features, and by allowing designs that ignite at lower drive energies.

Increasing the volumetric heating rate of the solid should give smoother surfaces. Absorbed radiation from an infrared laser provides this additional heating, allowing us to increase the heating thirty-fold over beta-heating, with the limit being set only by the available laser intensity [38]. This bulk heating can be applied to D_2 or HD solids, making it easier to experiment without the complications of using tritium. The technique has been applied to HD layers in polymer spheres by centering them in a diffusely reflecting integrating sphere into which the infrared is injected and symmetrized [39]. The layer smoothness achieved was comparable to that of beta layering in spheres, with a similar spectrum. To form layers by infrared absorption, the radiation wavelength has to be selected for the particular isotope or mixture, but is generally in the 2 to 3 micron range. There must also be a suitable transparency band in the capsule material. The plasma polymer ablator used for current Nova experiments has such a window, provided it is formed from fully deuterated organic monomers. Being applicable to non-tritiated fuel layers, such as D_2 or isotopic mixtures, this may be the only way to make sufficiently smooth layers of these materials, which could prove very useful in the pre-ignition phase of NIF experiments.

The cryogenic fuel layer must be uniformly thick to better than 1% to yield a sufficiently symmetric implosion. For this, the interface between the fuel layer and the spherical capsule must be isothermal to 15 μK at an average temperature of 18.5 K. For indirect-drive, the hohlraum is a mini-cryostat, with the heat from the beta-decay conducted to the wall, but the isotherms in an isothermal cylindrical hohlraum are not spherical, and in fact can severely distort the layer. However, a high thermal conductivity capsule ameliorates this problem which gives a another large advantage to beryllium. For plastics, on the other hand, the hohlraum boundary temperature must be tailored to provide spherical isotherms at the capsule. We are designing and testing hohlraums that will do this as in Fig 12. Azimuthally symmetric cooling will require specially designed contacts, as indicated in Fig 12. The axial temperature profile on the hohlraum wall will be maintained by microheaters on the hohlraum exterior. Thermal modeling [40] shows that a uniform surface heating flux very nearly produces the required thermal profile if the cooling rings are attached at the hohlraum ends with partial shielding as shown.

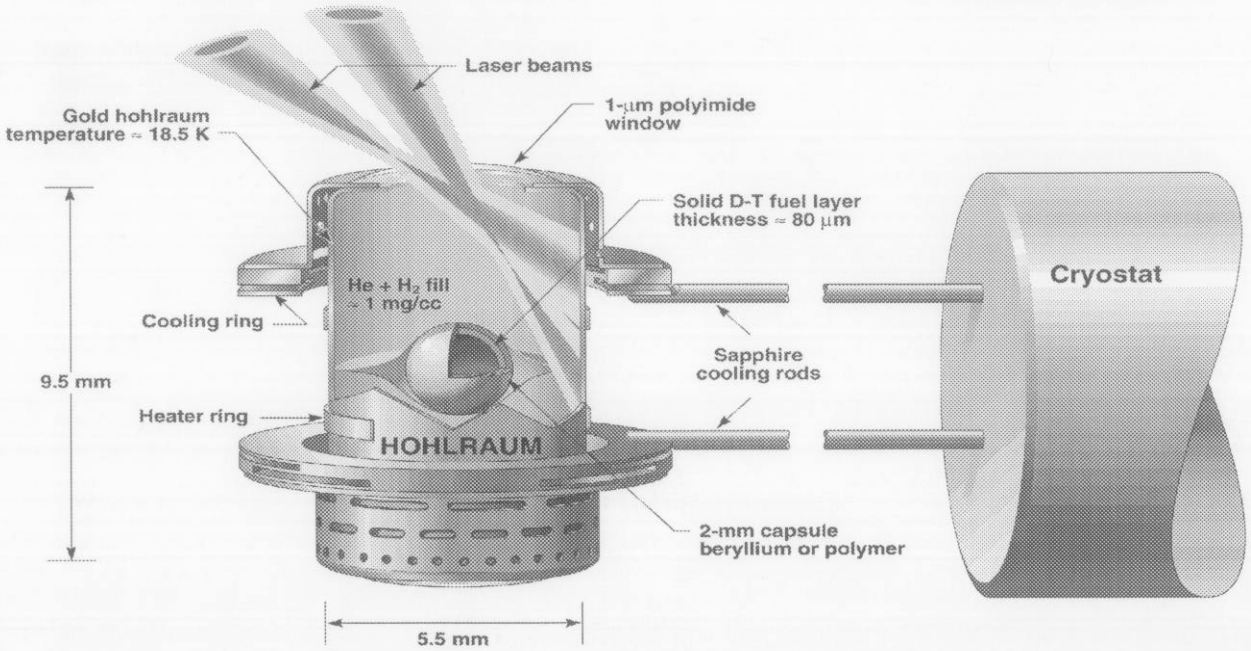

FIG. 12 Forming a uniformly thick fuel layer in a cryogenic ignition hohlraum will require very careful thermal control provided by the hohlraum.

---

† In collaboration with:

N. Alexander[6], P. Amendt[1], R. Berger[1], G. Besenbruch[6], D. Bittner[5], M.A. Blain[2], D. Bradley[3], E.M. Campbell[1], R. Cauble[1], P. Celliers[1], R. Chrien[4], G. Collins[1], M. Cray[4], E. Dattalo[2], N. Dague[2], C. Decker[1], R. Cook[1], L. DaSilva[1], N. Delameter[4], T. Dittrich[1], K. Estabrook[1], J. Fernandez[4], L. Foreman[4], C. Gibson[6], S.G. Glendinning[1], W. Giedt[1], S. Glenzer[1], A. Hauer[4], D. Hinkel[1], J. P. Jadaud[2], D. Kalantar[1], J. Knauer[3], R. Kauffman[1], J.D. Kilkenny[1], R. Kirkwood[1], W. Kruer[1], B. Lasinski[1], A.B. Langdon[1], J. Lindl[1], G. Magelssen[4], M. Marinak[1], F.J. Marshall[3], R. McCrory[3], M.C. Monteil[2], R. McEachern[1] W. Miller[6], J. Moody[1], D. Munro[1], T.J. Murphy[4], S. Pollaine[1], A. Richard[2], C. Roberts[1], H. Rose[4], J. Sanchez[1], J. Sater[5], W. Seka[3], K. Schultz[6], J.M. Soures[3], R. Stephens[6], R. Turner[1], C. Verdon[1], S. Weber[1], D. Wilson[4], E. Williams[1]

[1]Lawrence Livermore National Laboratory, Livermore, California 94551
[2]CEA, Centre de Bruyeres-le-Chatel, 91680 Bruyeres-le-Chatel, France
[3]Laboratory for Laser Energetics, University of Rochester, Rochester, New York 14627
[4]Los Alamos National Laboratory, Los Alamos, New Mexico 87545
[5]Schafer Corporation, Livermore, CA 94551
[6]General Atomics, San Diego, CA 92186

References

[1] HAAN, S.W., et al., Phys. Plasmas **3**, 2084 (1996).
[2] HAAN, S.W., et al., Phys. Plasmas **2**, 2480 (1995).
[3] BERGER, R.L., et al., Phys. Plasma, **3**, 2029 (1996).
[4] D.H. Kalantar, et al., Phys. Plasmas, Production and characterization of large plasmas from gasbag targets on Nova, **2**, 3161 (1995); B.J. MacGowan, et al., Phys of Plasmas, Laser-plasma

interactions in ignition-scale hohlraum plasmas, **3**, 2029 (1996); S. H. Glenzer, et al., Phys. Rev., Electron temperature and density measurements in large scale-length gasbag plasmas by K-shell spectroscopy, E **55**, 927-938 (1997).
[5] MACGOWAN, B.J., et al, these Proceedings.
[6] KAUFFMAN, R.L., et al., Phys. Rev. Lett. **73**, 2320 (1994).
[7] DECKER, C.D., et al., Phys. Rev. Lett., **79**, 1491 (1997).
[8] GLENZER, S.H., et al., Phys. Rev. Lett., **80**, 2845 (1998).
[9] DATTOLO, et al., to be published.
[10] KORNBLUM, H.N., et al., Rev. Sci. Instrum. **57**, 2179 (1986).
[11] LINDL, J.D., Physics of Plasmas **2**, 3933 (1995).
[12] HAAN, S.W., et al., Physics of Plasmas **2**, 2480 (1995).
[13] KAUFFMAN, R.L., et al., Physics of Plasmas **5**, 1927 (1998).
[14] SUTER, L.J., Lawrence Livermore National Laboratory, Diagnosing Capsule Drive Asymmetry via a Reemission Ball, UCRL-50055-84 (1984).
[15] HAUER, A.A, et al., Physics of Plasmas **2**, 2488 (1995).
[16] AMENDT, P., et al., Review of Scientific Instruments **66**, 785 (1995); P. Amendt, et al., Physics of Plasmas **4**, 1862 (1997).
[17] SUTER, L.J., et al., Physical Review Letters **73**, 2328 (1994).
[18] MURPHY, T.J., et al., Physics of Plasmas **5**, 1960 (1998).
[19] DELAMATER, N.D., et al., Physics of Plasmas **3**, 2022 (1996).
[20] GLENDINNING, S.G., et al., to be published in Review Scientific Instrum. (1999).
[21] TURNER, R.E., et al., submitted to Technical Review Letters (1998).
[22] GLENDINNING, S.G., et al., to be published in Review Scientific Instrum. (1999).
[23] LANDEN, O.L., et al., these Proceedings.
[24] GLENDINNING, S.G., et al., to be published in Review Scientific Instrum. (1999).
[25] LANDEN, O.L., et al., J. Quant. Spectrosc. Radiat. Transfer **54**, 245 (1995).
[26] MARINAK, M.M., et al., Physics of Plasmas **3**, 2070 (1996).
[27] COLLINS, G.W., et al., Science **281,** 1178 (1998).
[28] COLLINS, G.W., et al., submitted to Physical Review Letters.
[29] MARINAK, M.M., et al., Physics of Plasmas **5** (4), April, 1998.
[30] WILSON, D.C., et al., Physics of Plasmas **5** (5), May, 1998.
[31] MARGEVICIOUS, R.W., et al., to be published in J. Fusion Technology, March 1999
[32] MCEACHERN, R., et al., Fusion Technology **31**, 435 (1997)
[33] MCEACHERN, R., Alford, C., submitted to Fusion Technology.
[34] SANCHEZ, J.J., et al., Fusion Technology **31**, 491 (1997).
[35] ROBERTS, C.C., et al, "Polyimide Films from Vapor Deposition: Toward High Strength NIF Capsules," Fusion Tech (1999), in press.
[36] SATER, J., et al., submitted to Fusion Technology.
[37] HOFFER, J.K., et al., Fusion Technology **30**, 529, (1996).
[38] COLLINS, G.W., et al., J. Vac. Sci. Technol. A **14** (5), Sep/Oct 1996.
[39] BITTNER, D.N., et al., submitted to Fusion Technology.
[40] SANCHEZ, J.J., et al., submitted to Applied Physics (1998).